Title	Dynamic motion of two-link arms with different link lengths using singularities
Author(s)	Nakamura, Masashi; Urakubo, Takateru; Muromaki, Takao
Citation	The 11th International Symposium on Adaptive Motion of Animals and Machines (AMAM2023). 2023, p. 105-106
Version Type	VoR
URL	https://doi.org/10.18910/92289
rights	
Note	

Dynamic motion of two-link arms with different link lengths using singularities

Masashi Nakamura[1], Takateru Urakubo[1], Takao Muromaki[2]
[1]Graduate School of System Informatics, Kobe University, Japan
223x115x@stu.kobe-u.ac.jp, *t.urakubo@silver.kobe-u.ac.jp*
[2]Mechanical Engineering, National Institute of Technology, Maizuru College, Japan
t.muromaki@maizuru-ct.ac.jp

1 Introduction

Link mechanisms such as robot arms have postures called singular configurations. Humans use the singular configurations for dynamic movements. For example, in jumping, the legs extend in a straight line at the instant they leave the ground. In the case of Orthoptera jumping, the legs change from an almost fully folded posture to a posture almost extended in a straight line during the movement [1]. Assuming that the legs are a two-link mechanism, the postures completely folded and extended in a straight line are singular configurations. In addition, the lengths of upper and lower legs and their ratios vary among creatures. So the following questions arise; What are the advantages of the singular configurations? And what are the effects of different lengths between the two links?

In this paper, pulling motion of a two-link arm is considered to investigate the advantages of singular configurations and the effects of the different lengths between two links. The pulling motion that minimizes necessary joint torques is searched for by numerical optimization, and dynamic manipulability ellipsoids [2] are drawn on the obtained motion to discuss the advantages and the effects.

2 Pulling Motion of a Two-Link Arm

2.1 Two-Link Arm

As shown in Fig. 1, the pulling motion of a two-link arm holding a heavy weight with its end-effector on a horizontal plane is considered. The lengths, masses, and inertia of two links are l_1 and l_2, m_1 and m_2, and I_1 and I_2, respectively. The input torques at Joint 1 and Joint 2 are expressed as τ_1 and τ_2. The locations of the arm base and the end-effector are denoted as $p_b = [x_b, y_b]^T$ and $p_e = [x_e, y_e]^T$. The postures extended in a straight line and folded completely are singular configurations, which are denoted as the singular configuration s_1 and s_2, respectively.

2.2 Optimization Problem

At initial time $t = 0$ and end time $t = T$, the arm is assumed to be stationary. The initial and end locations of the weight are set to be $p_e(0) = [0,0]^T$ and $p_e(T) = [0, y_T]^T$, respectively. It is supposed that the location of the base is on the y-axis and the end-effector moves along the y-axis. Note that the posture during the motion depends on the base location y_b. Joint friction and gravity are not considered. The trajectory of end-effector $p_e(t)$ that minimizes the following cost function J_c is searched for at each base location y_b. Optimization is performed using MATLAB by representing $p_e(t)$ as spline functions of t.

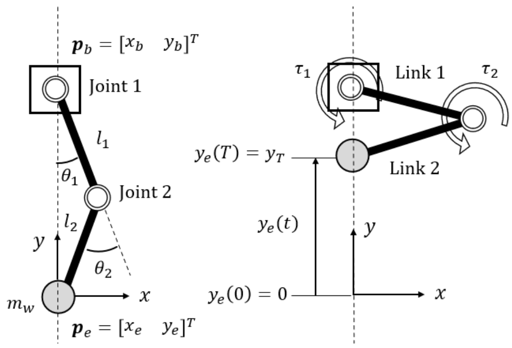

Figure 1: Two-link arm with a heavy weight.

$$J_c = \int_{t=0}^{t=T} (\tau_1^2 + \tau_2^2) dt \ . \tag{1}$$

3 Optimized Motion with Different Link Lengths

3.1 Numerical Setting

To examine the difference in J_c due to the lengths of two links, the following three settings are considered.
Setting A : $l_1 = l_2 = 0.5$ [m], $m_1 = m_2 = 1$ [kg]
Setting B : $l_1 = 0.4, l_2 = 0.6$ [m], $m_1 = 0.8, m_2 = 1.2$ [kg]
Setting C : $l_1 = 0.3, l_2 = 0.7$ [m], $m_1 = 0.6, m_2 = 1.4$ [kg]
In each setting, the inertia is set to be $I_1 = I_2 = 0.1$ [kgm^2], and the mass of the weight is chosen as $m_w = 50$ [kg]. The end time is set to be $T = 1$ [s], and the movement distance of end-effector is chosen as $y_T = 0.3$ [m].

The base location y_b is changed discretely, with an interval of 0.001 [m], in the range that does not result in an exact singular configuration during the motion. For Setting A, B, and C, the ranges of y_b are $[0.301, 0.999]$ [m], $[0.501, 0.999]$ [m], and $[0.701, 0.999]$ [m], respectively. In particular, cases of $y_b = 0.999$ [m] in Setting A, B, and C

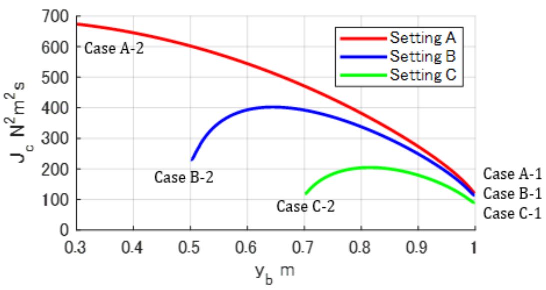

Figure 2: Variation of J_c with respect to y_b.

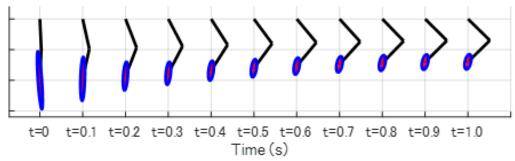

(a) Case A-1 ($y_b = 0.999$ [m], $J_c = 120.6$ [N^2m^2s])

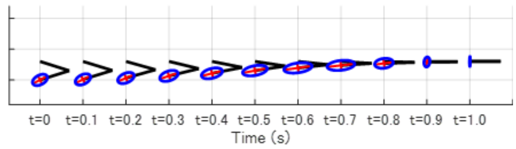

(b) Case A-2 ($y_b = 0.301$ [m], $J_c = 673.6$ [N^2m^2s])

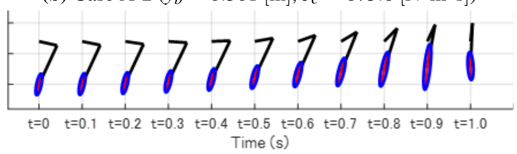

(c) Case C-2 ($y_b = 0.701$ [m], $J_c = 118.5$ [N^2m^2s])

Figure 3: Dynamic manipulability ellipsoid every 0.1 [s] in optimized motion.

are called Case A-1, B-1, and C-1, respectively. Also, cases of $y_b = 0.301$ [m] in Setting A, $y_b = 0.501$ [m] in Setting B, and $y_b = 0.701$ [m] in Setting C are called Case A-2, B-2, and C-2, respectively.

3.2 Results and Discussion

Fig. 2 shows the relationship between the base location y_b and the cost function J_c. In Fig. 3, the optimal motions of Case A-1, A-2, C-2 are drawn every 0.1 [s]. In addition, dynamic manipulability ellipsoids are drawn on the end-effectors. The dynamic manipulability ellipsoid represents the range of acceleration that the end-effector can produce within the joint torques that satisfy $\tau_1^2 + \tau_2^2 \leq 1$.

From Fig. 2, it can be seen that the shape of the graph for Setting A is considerably different from the others. The larger the difference between the lengths of the two links, the smaller the value of J_c, although the range of y_b becomes smaller. A smaller range of y_b means that the workspace of the end-effector is smaller. For Case A-1, B-1, and C-1, the values of J_c are 120.6 [N^2m^2s], 114.0 [N^2m^2s], and 91.7 [N^2m^2s], respectively, which are the minimum values in each Setting. In Case A-1 shown in Fig. 3 (a), the arm is extended almost in a straight line around the initial time, that is, near the singular configuration s_1. At that time, the dynamic manipulability ellipsoids are long in the y-axis direction. This means that the end-effector can accelerate more in the pulling direction near the singular configuration s_1 than in other postures. The optimal motions and dynamic manipulability ellipsoids in Case B-1 and C-1 are similar to those in Case A-1. From the above, it can be considered that the most efficient motion can be carried out by using the postures around the singular configuration s_1.

Next, we focus on Fig. 3 (b) and (c). In Fig. 3 (b), the dynamic manipulability ellipsoids are long in the x-axis direction around $t = 0.7$ [s], when the arm postures are near the singular configuration s_2. On the other hand, in Fig. 3 (c), the dynamic manipulability ellipsoids are long in the y-axis direction throughout the motion, and they become longer near the singular configuration s_2. That is, near the singular configuration s_2, it is easy to accelerate the heavy weight in Case C-2, while it is difficult in Case A-2. Also, dynamic manipulability ellipsoids in Case B-2 are similar to those in Case C-2. This suggests that only if there is a difference in length between the two links, it is possible to pull a heavy weight with less energy using the postures near the singular configuration s_2, and furthermore, the greater the difference, the less energy is consumed. This dynamic property near the singular configurations would explain the difference in shape between the three graphs in Fig. 2.

From the above discussion, animals including humans may use the singular configurations to perform dynamic movements because of the large dynamic manipulability in the movement direction. In addition, the different lengths between two links, such as human forearm and upper arm, enable energy saving motions, although the workspace becomes smaller.

4 Conclusion

The advantage of the singular configurations, which are used in dynamic motions unconsciously by animals including humans, was demonstrated for the pulling motion of a two-link arm. The optimal motions for three settings of link lengths were searched for within the allowable range of base location. Dynamic manipulability ellipsoids for the postures on the motions were drawn to check the ability to accelerate a heavy weight in the pulling direction. The weight can be accelerated efficiently by joint torques near the singular configuration s_1. The efficient acceleration can also be seen near the singular configuration s_2 only if there is a difference in length between the two links.

Acknowledgement This work was supported by JSPS KAKENHI Grant Number JP20K04350.

References

[1] M. Burrows, O. Morris, "Jumping and kicking in bush crickets," *Journal of Experimental Biology*, Vol. 206, Issue 6, pp. 1035–1049, 2003.

[2] T. Yoshikawa, "Dynamic manipulability of robot manipulators," *Proceedings. 1985 IEEE International Conference on Robotics and Automation*, pp. 1033–1038, 1985.